Journal of Medicinal Chemistry

Article

pubs.acs.org/jmc

Structure−Activity Relationship Studies of Sulfonylpiperazine Analogues as Novel Negative Allosteric Modulators of Human Neuronal Nicotinic Receptors

Brandon J. Henderson,[†] Daniel J. Carper,[∥] Tatiana F. González-Cestari,[†] Bitna Yi,[†] Kiran Mahasenan,[‡] Ryan E. Pavlovicz,[§] Martin L. Dalefield,[†] Robert S. Coleman,[∥] Chenglong Li,[‡,§] and Dennis B. McKay*[,†]

[†]Division of Pharmacology and [‡]Division of Medicinal Chemistry, College of Pharmacy, The Ohio State University, 500 West 12th Avenue, Columbus, Ohio 43210, United States

[§]Biophysics Program, The Ohio State University, Columbus, Ohio 43210, United States

[∥]Department of Chemistry, The Ohio State University, 88 West 18th Avenue, Columbus, Ohio 43210, United States

Supporting Information

ABSTRACT: Neuronal nicotinic receptors have been implicated in several diseases and disorders such as autism, Alzheimer's disease, Parkinson's disease, epilepsy, and various forms of addiction. To understand the role of nicotinic receptors in these conditions, it would be beneficial to have selective molecules that target specific nicotinic receptors in vitro and in vivo. Our laboratory has previously identified novel negative allosteric modulators of human $\alpha4\beta2$ (H$\alpha4\beta2$) and human $\alpha3\beta4$ (H$\alpha3\beta4$) nicotinic receptors. The effects of novel sulfonylpiperazine analogues that act as negative allosteric modulators on both H$\alpha4\beta2$ nAChRs and H$\alpha3\beta4$ nAChRs were investigated. This work, through structure−activity relationship (SAR) studies, describes the chemical features of these molecules that are important for both potency and selectivity on H$\alpha4\beta2$ nAChRs.

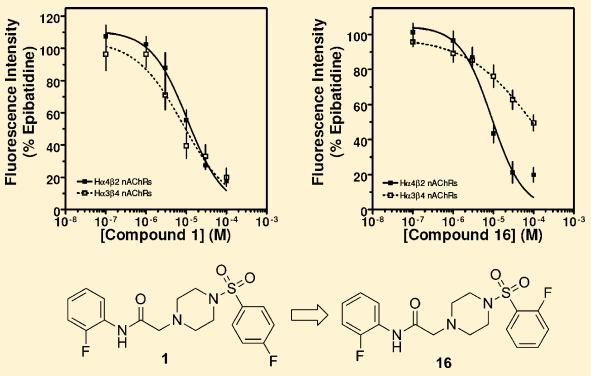

INTRODUCTION

Neuronal nicotinic acetylcholine receptors (nAChRs) are associated with many important physiological mechanisms (i.e., cognition, arousal, pain sensation), as well as a number of neurological diseases and disorders (depression, schizophrenia, Alzheimer's disease, Parkinson's disease, lung cancer, Tourette's syndrome, autism, and addiction).[1−4] nAChRs are notable for their implications in the addictive properties of nicotine, the primary addictive component of tobacco products.[5] nAChRs are ligand-gated ion channels composed of five protein subunits encoded by a family of related but distinct genes.[6,7] Multiple nAChR subtypes have been described based on subunit ($\alpha2-\alpha10$ and $\beta2-\beta4$) composition, where the three most prominent subtype compositions in the CNS are $\alpha4\beta2$, $\alpha3\beta4$, and $\alpha7$.[8] The specific nAChR subtypes involved with most of the above-mentioned physiological processes or diseases are not known, and their study is challenging because of the complex composition of some nAChRs ($\alpha4\alpha6\beta2$, $\alpha3\alpha5\beta4$, etc.).[9,10] Despite the lack of understanding concerning specific subtypes of nAChRs in diseases and disorders, it is widely accepted that nicotine addiction is mediated primarily by $\alpha4\beta2$ containing nAChRs.[11,12] The discovery of novel, selective molecules that target specific subtypes of nAChRs would contribute significantly to our understanding of the role nAChR subtypes play in normal and pathophysiological states and prove beneficial for the clinical treatment of several neuropathologies.

Worldwide, nicotine addiction is a significant problem. Smoking is the primary cause of preventable death worldwide, and roughly 90% of the people who attempt to quit are unable to do so.[13] Current FDA approved treatments for tobacco addiction are nicotine replacement, buproprion, and varenicline. Each of these therapies has a modest success of 20−30% abstinence 1 year after quit date.[14−16] The target site of many nAChR drug discovery programs is the orthosteric (agonist binding) site of nAChRs,[9,17] and few laboratories have had some success in identifying molecules that show some selectivity using this approach.[18,19] However, one difficulty with this strategy is the high degree of amino acid sequence homology among nAChR α and β subunits in the ligand binding domain for acetylcholine, making it difficult to develop drugs that specifically target nAChR subtypes.[9,17] Thus, the development of selective nAChR drugs directed at orthosteric sites progresses slowly. For this reason, drugs targeting "nonorthosteric" sites of nAChRs (e.g., allosteric, noncompetitive sites) is an approach now taken by many laboratories.[20−22]

Received: September 28, 2011
Published: November 7, 2011

Mecamylamine, a nonselective noncompetitive nAChR antagonist, was shown to promote 40% abstinence at the year mark when used as an agonist−antagonist therapy in combination with the nicotine patch.[23] In addition, antagonists of $\alpha4\beta2$ nAChRs block nicotine self-administration on fixed and progressive ratio schedules in rats.[20,24] These data support the use of antagonists as nicotine cessation therapies; however, to produce new therapeutic molecules, it has widely been accepted that nAChR subtype selectivity must be pursued.[9] Selectivity is especially important for avoiding effects on $\alpha3\beta4$ nAChRs, as they are the prominent nAChR subtype in the peripheral nervous system.[9,10] Furthermore, it has been postulated that this nAChR subtype mediates many of the adverse affects associated with therapeutics that target nAChRs.[14,23] Our laboratory has identified a novel allosteric site on H$\alpha4\beta2$ nAChRs that is approximately 10 Å from the orthosteric site at the interface of the α and β subunits.[25] This site was identified through a combination of homology modeling, blind docking, and molecular dynamics studies and was confirmed through the use of site-directed mutagenesis.[25,26] At this site, a novel class of NAMs has been shown to have relative selectivity for H$\alpha4\beta2$ nAChRs (over H$\alpha3\beta4$ nAChRs) principally through nonconserved amino acids on the $\beta2$ subunit. Through SAR we have identified several physiochemical features that mediate relative selectivity for H$\alpha4\beta2$ nAChRs. These include specific placement of aromatic residues, specific orientation of the keto group of esters or amides, and the specific length of carbon chains. By use of the allosteric site that was identified through computational modeling,[25,26] a small library of diverse molecules were computationally docked to identify novel chemical scaffolds that are active as nAChR NAMs. This structure-based virtual screening (SBVS) approach resulted in the identification of four novel scaffolds that show preference for H$\alpha4\beta2$ nAChRs and act as inhibitors of nAChRs.[27] One of these SBVS hits has a sulfonylpiperazine scaffold unique among previously described nAChR NAMs. Here in these studies we present the SAR of novel sulfonyl analogues on H$\alpha4\beta2$ and H$\alpha3\beta4$ nAChRs and describe the physical and chemical features that are important for both relative selectivity and potency on H$\alpha4\beta2$ nAChRs.

CHEMISTRY

We have previously reported that SBVS has yielded active hits that target H$\alpha4\beta2$ nAChRs.[27] A hit molecule (**1**) has been selected as a scaffold for the development of a focused library of compounds. Lead compound **1** was assembled through a convergent synthesis allowing for facile access to analogues. Retrosynthetically, compound **1** was formed from displacement of bromide **2** by arylsulfonylpiperazine **3** (Scheme 1). The two coupling partners were assembled from commercially available starting materials, where amide **2** resulted from acylation of *o*-fluoroaniline (**4**) with bromoacetyl bromide (**5**) and where piperazine **3** resulted from sulfonylation of piperazine (**6**) with *p*-fluorobenzenesulfonyl chloride (**7**).

This synthetic plan allowed access to a small library of compounds simply by using various substituted anilines and arylsulfonyl chlorides. Analogues were thus available in two linear steps (three total) from commercially available reagents. In practice, the synthetic plan was executed as planned where *o*-fluoroaniline (**4**) was acylated with bromoacetyl bromide (**5**) in the presence of triethylamine to yield amide **2** (Scheme 2).[28] In addition to *o*-fluoroaniline (**4**), five other aniline derivatives, 3-aminopyrazole, and *o*-phenylphenol were reacted in a similar manner to access a variety of α-bromoamides and an α-bromoester in unoptimized yields ranging from 26% to 96%.[29]

Scheme 1. Retrosynthetic Analysis of Lead Compound 1

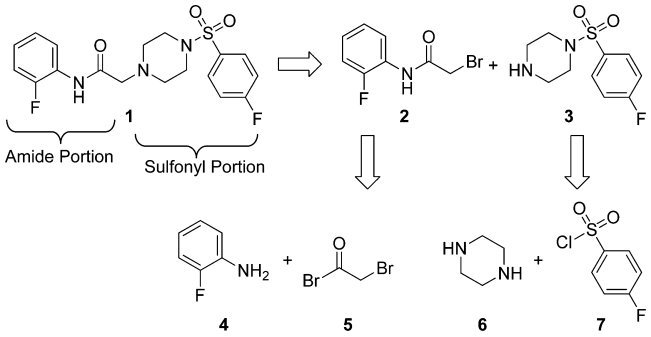

Scheme 2. Synthesis of Left Hand α-Bromoamides

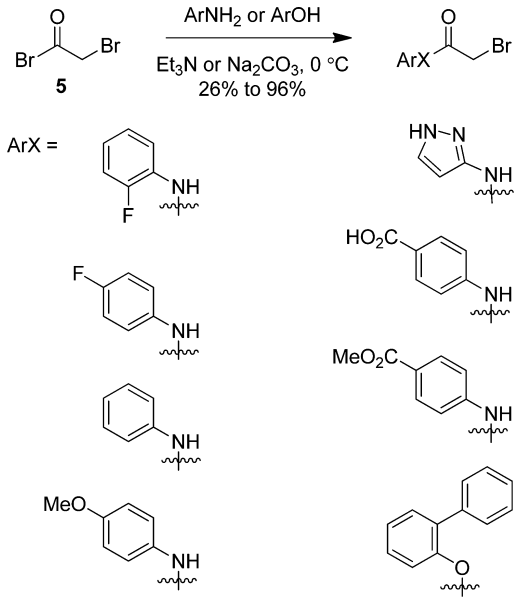

The piperazine fragment **3** was obtained in high yield from the reaction of *p*-fluorobenzenesulfonyl chloride with excess piperazine (Scheme 3).[30] Four other arylsulfonyl chlorides were reacted with piperazine to obtain the arylsulfonylpiperazine right-hand fragments needed to assemble analogues.

Scheme 3. Synthesis of Right Hand Arylsulfonylpiperazines

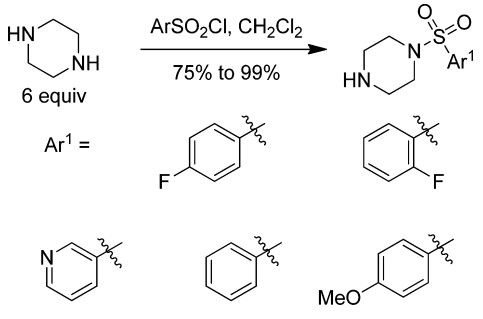

With the left side bromide (**2**) and right side piperazine (**3**) in hand, the two fragments were coupled in the presence of sodium carbonate to obtain lead compound **1** (Scheme 4). The various other left and right side fragments were mixed and

dx.doi.org/10.1021/jm201294r | J. Med. Chem. 2011, 54, 8681–8692

Scheme 4. Coupling of Left Side Bromide with Right Side Piperazine

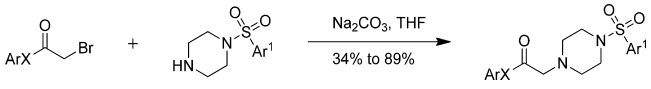

matched to obtain analogues **12**–**30** (Tables 1–5) in unoptimized yields varying from 34% to 89%.

The only analogue not accessible through this convergent method was aminoindazole analogue **11**. The inability to cleanly acylate 5-aminoindazole (**10**) with bromoacetyl bromide (**5**) led to a linear approach to obtain aminoindazole **11**. To this end, bromoacetic acid (**8**) was reacted in the presence of triethylamine with *p*-fluorobenzenesulfonylpiperazine (**3**) to provide acid **9**. Standard amide coupling conditions (EDCI, HOBt) were then employed to obtain analogue **11** in modest 46% yield (Scheme 5).[31]

Scheme 5. Linear Synthesis of Aminoindazole 11

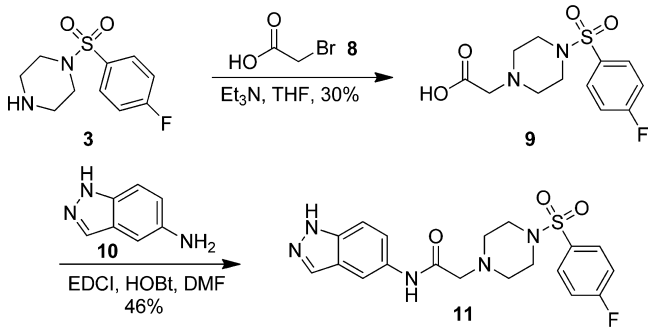

RESULTS

Series 1 SAR. Lead compound **1** produced inhibition on both H$\alpha 4\beta 2$ and H$\alpha 3\beta 4$ nAChRs with IC_{50} values of 9.3 and 9.0 μM, respectively (Table 1). The right side *p*-fluorobenzene-

Table 1. Series 1 SAR Studies

	Hα4β2 nAChRs		Hα3β4 nAChRs	
Compound	**IC_{50} Value (μM)[a]**	**n_h[b]**	**IC_{50} Value (μM)[a]**	**n_h[b]**
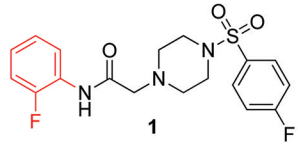 **1**	9.3 (6.2-13.9)	-1.2	9.0 (6.3-12.9)	-1.2
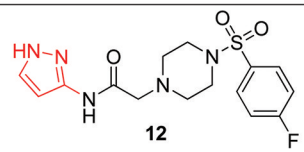 **12**	>100[c]	~	>100[c]	~
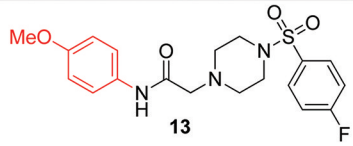 **13**	21.1 (15.7-28.4)	-0.9	29.6 (18.9-46.3)	-1.1
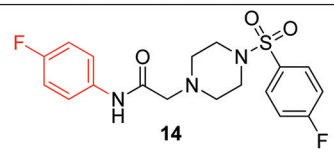 **14**	13.8 (10.7-17.8)	-0.9	11.6 (5.5-24.5)	-1.1
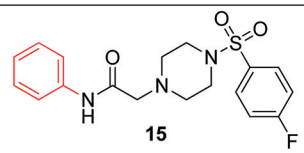 **15**	14.9 (11.5-19.4)	-1.4	18.5 (15.6-21.9)	-1.2
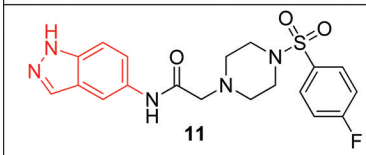 **11**	6.6 (3.8-11.3)	-1.0	23.8 (13.1-43.3)	-0.8

[a]Values represent geometric mean (confidence limits), n = 5–10. [b]n_h, Hill coefficient. [c]No activity up to 100 μM.

dx.doi.org/10.1021/jm201294r | J. Med. Chem. 2011, 54, 8681–8692

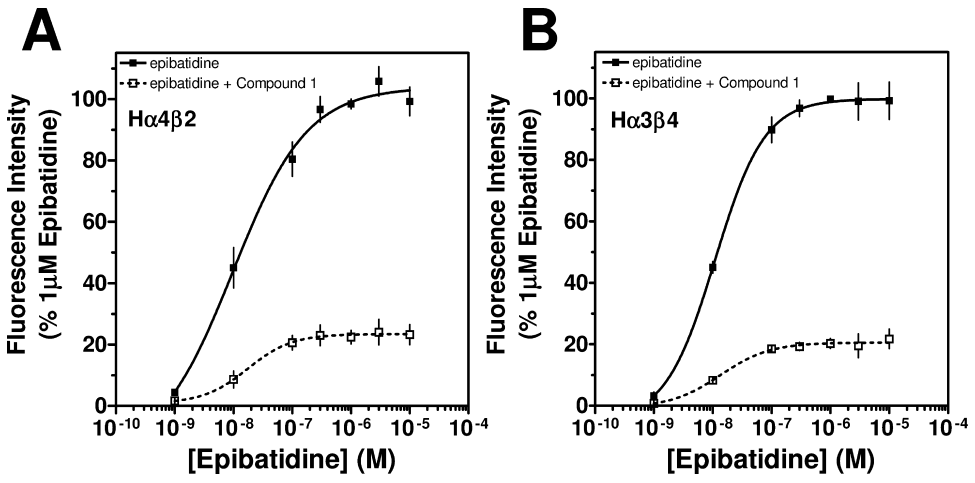

Figure 1. Concentration–response effects of epibatidine in the absence and presence of compound **1**. Calcium accumulation assays were performed as described in the methods section. The concentration–response effects of ebibatidine were investigated in the absence (■) or presence (□) of 30 μM **1** (~IC_{70}) by using HEK ts201 cells expressing H$\alpha4\beta2$ nAChRs (A) and H$\alpha3\beta4$ nAChRs (B). Values represent the mean ± SEM (n = 4).

Table 2. Series 2 SAR Studies

	Hα4β2 nAChRs		Hα3β4 nAChRs	
Compound	**IC_{50} Value (μM)[a]**	**n_h[b]**	**IC_{50} Value (μM)[a]**	**n_h[b]**
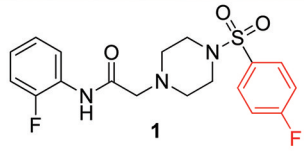 **1**	9.3 (6.2-13.9)	-1.2	9.0 (6.3-12.9)	-1.2
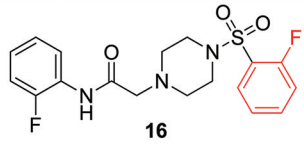 **16**	8.0 (5.4-11.8)	-1.5	99.8 (57.2-174)	-0.6
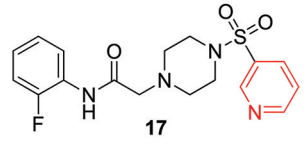 **17**	20.3 (12.6-32.6)	-1.1	49.6 (41.5-59.3)	-0.8
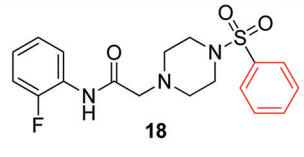 **18**	4.1 (3.0-5.7)	-1.4	4.0 (3.2-6.8)	-1.3
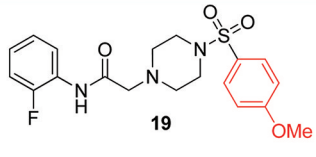 **19**	13.4 (9.8-18.4)	-1.3	15.4 (11.2-21.1)	-1.4

[a]Values represent geometric mean (confidence limits), n = 5–10. [b]n_h, Hill coefficient.

sulfonylpiperazine (**3**) had no effect on either H$\alpha4\beta2$ or H$\alpha3\beta4$ nAChRs (data not shown). When tested for competitive or noncompetitive activity on H$\alpha4\beta2$ and H$\alpha3\beta4$ nAChRs, lead compound **1** reduced the maximum efficacy for the agonist epibatidine (Figure 1). If the compounds acted at the agonist binding site, they would compete directly with the agonist, epibatidine, at its binding. This would produce a parallel shift of the concentration–response curve to the right. Compound **1** did not cause a parallel shift but instead decreased the maximum efficacy of epibatidine. According to

dx.doi.org/10.1021/jm201294r | J. Med. Chem. 2011, 54, 8681–8692

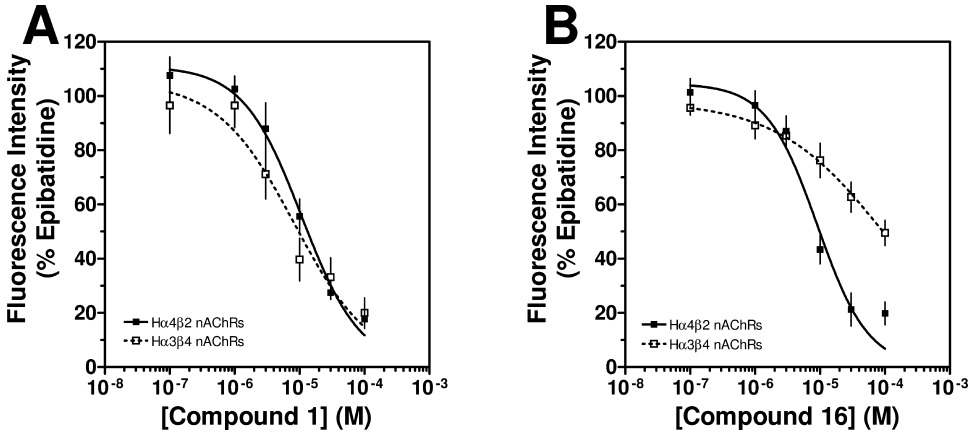

Figure 2. Concentration–response effects of compounda **1** and **16** on H$\alpha4\beta2$ and H$\alpha3\beta4$ nAChRs. Calcium accumulation assays were performed as described in the methods section. The concentration–response effects of compound **1** (A) and compound **16** (B) were investigated on H$\alpha4\beta2$ nAChRs (■) and H$\alpha3\beta4$ nAChRs (□). Values are the mean ± SEM (n = 6–9). IC_{50} values of compounds **1** and **16** are reported together in Table 2.

Table 3. Series 3 SAR Studies

	Hα4β2 nAChRs		Hα3β4 nAChRs	
Compound	**IC_{50} Value (μM)[a]**	**n_h[b]**	**IC_{50} Value (μM)[a]**	**n_h[b]**
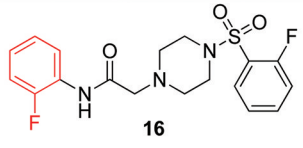 **16**	8.0 (5.4-11.8)	-1.5	99.8 (57.2-174)	-0.6
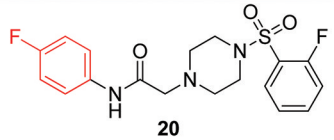 **20**	8.0 (4.5-14.3)	-1.2	13.6 (8.4-22.1)	-1.1
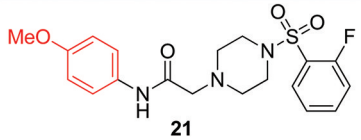 **21**	17.1 (14.1-20.7)	-1.0	19.1 (16.0-20.7)	-1.2
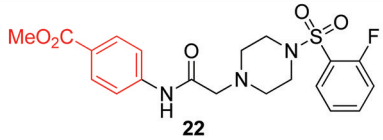 **22**	12.4 (8.8-17.6)	-1.1	11.2 (8.6-14.7)	-1.1
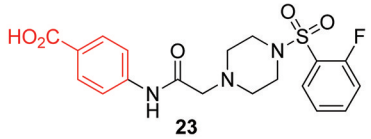 **23**	>100[c]	~	>100[c]	~
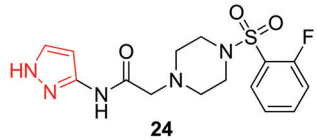 **24**	>100[c]	~	>100[c]	~

[a]Values represent geometric mean (confidence limits), n = 6–12. [b]n_h, Hill coefficient. [c]No activity up to 100 μM.

dx.doi.org/10.1021/jm201294r | J. Med. Chem. 2011, 54, 8681–8692

Table 4. Series 4 SAR Studies

	Hα4β2 nAChRs		Hα3β4 nAChRs	
Compound	**IC_{50} Value (μM)[a]**	**n_h[b]**	**IC_{50} Value (μM)[a]**	**n_h[b]**
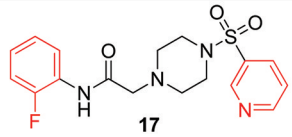 **17**	20.3 (12.6-32.6)	-1.1	48.9 (29.1-82.1)	-0.8
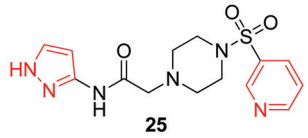 **25**	83.0 (48.3-143)	-0.5	>100[c]	~
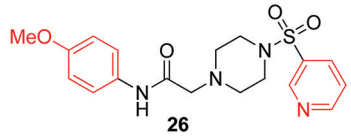 **26**	>100[c]	~	95.0 (74.0-122)	-1.5
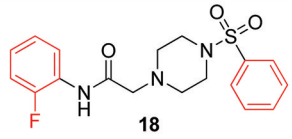 **18**	4.1 (3.0-5.7)	-1.4	4.6 (3.2-6.8)	-1.4
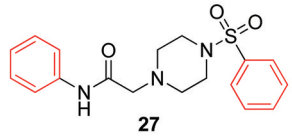 **27**	9.6 (6.0-15.2)	-0.9	16.4 (9.2-29.6)	-1.0
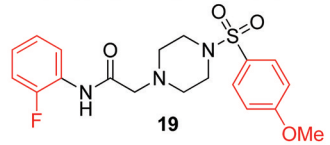 **19**	13.4 (9.8-18.4)	-1.3	15.4 (11.2-21.1)	-1.4
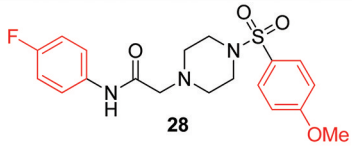 **28**	23.8 (20.6-27.5)	-1.0	17.1 (12.7-23.0)	-1.0

[a]Values represent geometric mean (confidence limits), n = 5−10. [b]n_h, Hill coefficient. [c]No activity up to 100 μM.

classical drug receptor theory, this result is indicative of noncompetitive inhibition (e.g., the binding at a site other than the agonist site). Therefore, this result suggests that compound **1** modulates nAChRs from an allosteric site. As outlined in the section Chemistry, analogues of **1** were synthesized. None of the compounds described here showed agonist activity on either H$\alpha4\beta2$ or H$\alpha3\beta4$ nAChRs in the calcium accumulation assay (data not shown).

In the first series of analogues, the amide portion of lead compound **1** was modified using several different substitutions (Table 1). This study was conducted to determine the synthetic flexibility of the amide portion and to determine how these changes effect potency on nAChRs. The pyrazole analogue (**12**) produced a significant decrease in potency for both H$\alpha4\beta2$ and H$\alpha3\beta4$ nAChRs (IC_{50} > 100 μM, Table 1). The methoxy analogue (**13**) produced a 2-fold decrease in potency for H$\alpha4\beta2$ nAChRs (IC_{50} = 21.1 μM, Table 1) and a 3-fold decrease in potency for H$\alpha3\beta4$ nAChRs (IC_{50} = 29.6 μM, Table 1). The *p*-fluorophenyl analogue (**14**) produced no significant change in potency for either H$\alpha4\beta2$ or H$\alpha3\beta4$ nAChRs (Table 1). The benzyl analogue (**15**) showed no significant change in potency on H$\alpha4\beta2$ nAChRs but showed a 2-fold decrease in potency for H$\alpha3\beta4$ nAChRs (IC_{50} = 18.5 μM, Table 1). The indazole analogue (**11**) produced a slight increase in potency for H$\alpha4\beta2$ nAChRs (IC_{50} = 6.6 μM, Table 1) and a 3-fold decrease in potency for H$\alpha3\beta4$ nAChRs (IC_{50} = 23.8 μM, Table 1).

dx.doi.org/10.1021/jm201294r | *J. Med. Chem.* 2011, 54, 8681–8692

Table 5. Series 5 SAR Studies

	Hα4β2 nAChRs		Hα3β4 nAChRs	
Compound	IC_{50} Value (μM)[a]	n_h[b]	IC_{50} Value (μM)[a]	n_h[b]
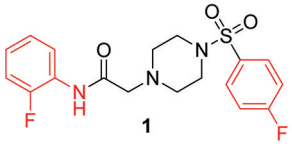 1	9.3 (6.2-13.9)	-1.2	9.0 (6.3-12.9)	-1.2
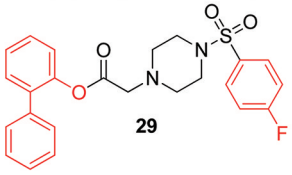 29	12.2 (6.3-23.8)	-1.1	23.8 (13.1-43.3)	-0.9
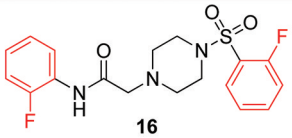 16	8.0 (5.4-11.8)	-1.5	99.8 (57.2-174)	-0.6
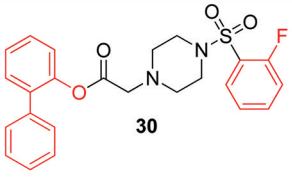 30	20.9 (12.7-34.3)	-1.2	23.5 (20.3-27.2)	-1.1

[a]Values represent geometric mean (confidence limits), n = 5−9. [b]n_h, Hill coefficient.

Series 2 SAR. In the next series of analogues, the sulfonyl portion of scaffold **1** was modified using several different substitutions (Table 2). Similar to the series 1 study, this was conducted to determine the synthetic flexibility of the sulfonyl portion and to determine how these changes affect potency on nAChRs. Movement of the fluorine from the para position (**1**) to the ortho position (**16**) produced no significant change in potency for Hα4β2 nAChRs; however, it resulted in a significant 12-fold decrease in potency for Hα3β4 nAChRs (IC_{50} = 99.8 μM, p < 0.01, Table 2). The pyridinyl analogue (**17**) produced a 2-fold decrease in potency for the Hα4β2 nAChR and a 5-fold decrease in potency for the Hα3β4 nAChR (IC_{50} of 20.3 and 49.6 μM, respectively, Table 2). The phenyl analogue (**18**) produced a 2-fold increase in potency for Hα4β2 and Hα3β4 nAChRs (IC_{50} of 4.1 and 4.0 μM, respectively, Table 2). The *p*-methoxyphenyl analogue (**19**) resulted in no significant change in potency for both Hα4β2 and Hα3β4 nAChRs (Table 2). From examination of the inhibition curves of **1** and **16** on nAChRs, **1** produces similar hill coefficients on both Hα4β2 and Hα3β4 nAChRs (Figure 2 and Table 2). **16** produces a similar hill coefficient as **1** on Hα4β2 nAChRs (n_h = −1.5) but produced a statistically significant (p < 0.0005) 2-fold decreased Hill coefficient on Hα3β4 nAChRs (n_h = −0.6, Table 2).

Series 3 SAR. In this series, analogue **16** (Table 2) was used as the basis of comparison. Replacement of the *o*-fluorophenyl with the *p*-fluorophenyl (**20**) resulted in no change in potency for Hα4β2 nAChRs (Table 3) and a 6-fold increase in potency for Hα3β4 nAChRs (IC_{50} = 13.6 μM, Table 3). Replacement of the *o*-fluorophenyl with a *p*-methoxyphenyl (**21**) resulted in a 2-fold decrease in potency for Hα4β2 nAChRs (IC_{50} = 17.1 μM, Table 3) and a 4-fold increase in potency for Hα3β4 nAChRs (IC_{50} = 19.1 μM, Table 3). Substitution of a methyl ester at the para position (**22**) resulted in no significant change for Hα4β2 and an 8-fold increase in potency for Hα3β4 nAChRs (IC_{50} = 11.2 μM, Table 3). Replacement of the fluorine with carboxylic acid (**23**) or instillation of a pyrazole heterocycle in place of the fluorophenyl (**24**) resulted in a loss of activity on both subtypes (Table 3).

Series 4 SAR. Pyridinyl, phenyl, and *p*-methoxyphenyl containing analogues of **1** were synthesized. The *o*-fluorophenyl, pyridinyl analogue (**17**) resulted in IC_{50} values of 20.3 and 48.9 μM on Hα4β2 and Hα3β4 nAChRs, respectively (Table 4). The pyrazole, pyridinyl analogue (**25**) resulted in IC_{50} values of 83.0 and >100 μM on Hα4β2 and Hα3β4 nAChRs, respectively (Table 4). The *p*-methoxyphenyl, pyridinyl analogue (**26**) resulted in a significant decrease in potency for both Hα4β2 and Hα3β4 nAChRs (IC_{50} values of >100 and 95.0 μM respectively, Table 4). The *o*-fluorophenyl, phenyl analogue (**18**) resulted in IC_{50} values of 4.1 and 4.6 μM on Hα4β2 and Hα3β4 nAChRs, respectively (Table 4). The phenyl, phenyl analogue (**27**) resulted in IC_{50} values of 9.6 and 16.4 μM on Hα4β2 and Hα3β4 nAChRs, respectively (Table 4). The *o*-fluorophenyl, *p*-methoxyphenyl analogue (**19**) resulted in no significant change in potency for both Hα4β2 and Hα3β4 nAChRs (Table 4). The *p*-fluorophenyl, *p*-methoxyphenyl analogue (**28**) resulted in a 2-fold decrease in

dx.doi.org/10.1021/jm201294r | J. Med. Chem. 2011, 54, 8681−8692

potency for both H$\alpha4\beta2$ and H$\alpha3\beta4$ nAChRs (IC_{50} values of 23.6 and 17.1 μM, respectively, Table 4).

Series 5 SAR. Biphenyl ester analogues were made of lead molecule **1** (**29**) and **16** (**30**). Biphenyl ester **29** showed no change in potency for H$\alpha4\beta2$ nAChRs and a 2-fold decrease in potency for H$\alpha3\beta4$ nAChRs (IC_{50} = 23.8, Table 5) compared to **1**. Biphenyl ester **30** showed a decrease in potency for H$\alpha4\beta2$ nAChRs (IC_{50} = 20.9 μM, Table 5) and a 3-fold increase in potency for H$\alpha3\beta4$ nAChRs (IC_{50} = 23.5, Table 5) in comparison to **16**.

DISCUSSION AND CONCLUSION

We understand that there are a multitude of nAChR subtypes and that a study such as this, utilizing only two subtypes, cannot use the term "selectivity" accurately. For this reason, the term "relative selectivity" has been used to describe the difference between only H$\alpha4\beta2$ and H$\alpha3\beta4$ nAChRs. The most significant change in series 1 was the pyrazole (**12**) modification, which abolished activity (up to 100 μM) for both subtypes. Movement of the fluorine led to no significant change; therefore, this suggests that the fluorine is not a significant contributor to selectivity or potency for this scaffold. Substitution of the indazole (**11**) did not affect potency on H$\alpha4\beta2$ nAChRs but decreased potency on H$\alpha3\beta4$. This suggests that this structure or position of the scaffold is amenable to optimization for H$\alpha4\beta2$ nAChR selectivity.

The significant findings of series 2 were that the *o*-fluorophenyl and pyridinyl substitutions showed an improvement in the relative selectivity for H$\alpha4\beta2$ nAChRs (9-fold and 3-fold, respectively). This result suggests that this position of the scaffold may improve the range of selectivity with further modification. Moving the fluorine from the para (**1**) to the ortho (**16**) positions may cause rotation of the ring due to proximity to the sulfonyl oxygen groups.

Series 3 data suggest that these substitutions have little effect on the potency of these molecules on H$\alpha4\beta2$ nAChRs (with the exception of pyrazole **24**); yet every change showed a decrease in relative selectivity for H$\alpha4\beta2$ nAChRs. The results of the comparison between analogues **20** and **16** (Table 3) contradict earlier results (e.g., the comparison between analogues **14** and **1**, Table 1). The first comparison showed that the fluorine position, ortho or para, had no effect on potency for H$\alpha3\beta4$ nAChRs (Table 1). However, we noticed that movement of the fluorine (**20** and **16**) makes a significant difference on potency for H$\alpha3\beta4$ nAChRs (Table 3). This suggests that this portion of the molecule is interacting at a different position in the ligand binding domain depending on the fluorine position on the phenyl of the sulfonyl portion. Compound **12** (series 1) and compound **24** both contained pyrazole moieties and resulted in a loss of activity on both nAChR subtypes. This suggests that more hydrophilic substitutions decrease binding and/or efficacy on nAChRs.

In pyridinyl analogues of series 4, the methoxybenzyl substitution to the amide portion (**26**) produced a significant change in potency on both subtypes (Table 4). This is surprising considering that similar substitutions had little effect on potency (**13** in Table 1 and **21** in Table 3). These data also show that other aromatics, such as a pyrazole, drastically reduce potency on nAChRs (**25**). In both the phenyl and *p*-methoxyphenyl analogues, molecules with fluorine substitutions at the ortho position (**18** and **19**) showed improved H$\alpha4\beta2$ nAChR potency compared to molecules that lacked a fluorine substitution (**27**) or had a fluorine substitution at the para position (**28**). This suggests that the ortho position is preferred for H$\alpha4\beta2$ nAChR potency.

Previously published data[25] showed that the incorporation of biphenyl structures is important for selectivity of molecules targeting H$\alpha4\beta2$ nAChRs. Therefore, biphenyl analogues of **1** and **16** were made in series 5. It was hypothesized that the ester carbonyl and fluorinated phenyl groups would act in a similar way as the ester and phenylpropyl of KAB-18.[25] However, these features found in this novel scaffold lack the flexibility of the phenylpropyl in KAB-18-like molecules and therefore may have a different binding mode within the binding site.

In conclusion, the SAR of sulfonylpiperizine analogues on H$\alpha4\beta2$ and H$\alpha3\beta4$ nAChRs has been described here. Compound **16** showed the highest relative selectivity for H$\alpha4\beta2$ nAChRs (12-fold, Table 3), while **18** showed the highest potency (Table 4) among the compounds described here. The SAR of these compounds has identified that the position of fluorine substitution on the sulfonyl portion (ortho vs para) has a significant effect on relative selectivity for H$\alpha4\beta2$ nAChRs. In these analogues, relative selectivity for H$\alpha4\beta2$ nAChRs is associated with *o*-fluorophenyl (**16**) while *p*-fluorobenzenes show no preference for H$\alpha3\beta4$ or H$\alpha4\beta2$ nAChRs. Additionally, the ortho substitution of halogens in the amide portion has shown improvement in potency for H$\alpha4\beta2$ nAChRs. In the future discovery of novel H$\alpha4\beta2$ nAChR antagonists, it would be informative to incorporate both of these features in the design of new NAMs to improve both potency and selectivity. Compounds **11** and **16**, which have modifications to the amide and sulfonyl positions, respectively, both led to an increase in selectivity for H$\alpha4\beta2$ nAChRs. Further studies may include making both modifications in a single molecule to improve selectivity for H$\alpha4\beta2$ nAChRs.

The structural diversity of these new analogues provides additional insight into the physiochemical features that are important for antagonism of nAChRs at allosteric sites. As mentioned before, the discovery of selective molecules targeting nAChRs has been slow. Studies like these contribute to the discovery and development of selective compounds that can be used as novel therapeutics for nAChR related diseases and disorders.

EXPERIMENTAL SECTION

Materials. Calcium 5NW dye was obtained from Molecular Devices (Sunnyvale, CA). Dulbecco's modified Eagle medium (DMEM), penicillin, streptomycin, and L-glutamine were obtained from Invitrogen Corporation (Grand Island, NY). Epibatidine was purchased from Sigma-Aldrich (St. Louis, MO). All other reagents were purchased from Fisher Scientific (Pittsburgh, PA). For pharmacological evaluation, all compounds were initially dissolved in 100% DMSO (0.01 M stocks). Stock solutions of compounds at concentrations less than or equal to 100 μM were made in HBK buffer.

Calcium Accumulation Assays. A procedure previously reported by our laboratory[25,32,33] was used with minor modifications. For the calcium accumulation assays, HEK ts201 cells stably expressing either H$\alpha4\beta2$ nAChRs or H$\alpha3\beta4$ nAChRs (obtained from Professor Jon Lindstrom, University of Pennsylvania, Philadelphia, PA) were used. Cells were plated at a density of (2.0−2.3) × 10^5 cells per well in clear 96-well culture plates previously coated with poly-L-ornithine. On the day of the experiment (typically ~24 h later), cells were washed (100 μL) with HEPES-buffered Krebs (HBK) solution[25,32,33] and incubated (protected from light) for 1 h at 24 °C with 50% Calcium 5 NW dye (Molecular Devices, Sunnyvale, CA). The plates were then placed into a fluid handling integrated fluorescence plate reader (FlexStation II, Molecular Devices, Sunnyvale, CA). Fluorescence was

read at excitation of 485 nm and emission of 525 nm from the bottom of the plate, and changes in fluorescence were monitored at ~1.5 s intervals. Inhibition curves were obtained in the concentration−response studies using six concentrations within a range of 0.1−100 μM for each compound reported here. Results are reported as IC_{50} values (see Tables 1−5). Results were expressed as a percentage of control, 1 μM epibatidine group. Because of solubility problems, compound concentrations greater than 100 μM were not used in our concentration−response studies. Therefore, compounds that showed no inhibition up to the highest concentration have been labeled with IC_{50} values of ">100" (see Tables 1−4). The DMSO concentration at this compound concentration was 1% and had no effect on basal or agonist-induced increases in fluorescence intensity.

Calculations and Statistics. Functional data were calculated from the number of observations (n) performed in triplicate. Curve fitting was performed by Prism software (GraphPad, San Diego, CA) using the equation for a single-site sigmoidal dose−response curve with a variable slope. IC_{50} values are expressed as geometric mean values (95% confidence limits). When statistical significance was calculated, the t test was used. Where data were labeled "not significant" or when "no significant difference" was reported, then $p > 0.05$.

General Chemistry Methods. ^{1}H (500 or 400 MHz) and ^{13}C (126 or 101 MHz) NMR spectra were recorded on a Bruker DRX-500 or Bruker DPX-400 spectrometer in $CDCl_3$ using $CHCl_3$ (^{1}H δ 7.26) and $CDCl_3$ (^{13}C δ 77.0) or DMSO-d_6 using DMSO (^{1}H δ 2.49) and DMSO-d_6 (^{13}C δ 39.51) as internal standards. High resolution mass spectra were recorded on a Bruker MicrOTOF ESI spectrometer provided by OBIC. Elemental analyses were carried out by Galbraith Laboratories, Inc. (Knoxville, TN). All reactions were conducted in either oven-dried (120 °C) glassware or flame-dried glassware, under an N_2 atmosphere when necessary. Tetrahydrofuran (THF) was distilled from benzophenone ketyl. Triethylamine and CH_2Cl_2 were distilled from calcium hydride prior to use. All other chemicals were used as received. All compounds were >95% pure as determined by elemental analysis (C, H, N), unless otherwise noted.

Synthesis. Preparation of *N*-Aryl-2-bromoacetamides. General Procedure A. Bromoacetyl bromide (10 mmol, 1 equiv) was added dropwise over 5 min to a solution of amine or alcohol (10 mmol, 1 equiv) and triethylamine (11 mmol, 1.1 equiv) in dichloromethane (50 mL, 0.2 M) at 0 °C. The reaction mixture was stirred at 0 °C for 20 min to 1 h, diluted with dichloromethane (50 mL), washed with saturated NH_4Cl (3 × 30 mL), dried (Na_2SO_4), and concentrated in vacuo to afford crude product. The crude product was purified by flash column chromatography, crystallization, or trituration to yield pure *N*-aryl-2-bromoacetamide (26−96%).

Preparation of Arylsulfonylpiperazines. General Procedure B. Arylsulfonyl chloride (10 mmol, 1 equiv) was added in one portion to a solution of piperazine (60 mmol, 6 equiv) in CH_2Cl_2 (100 mL, 0.1 M) at 0 °C. The reaction mixture was stirred at 0 °C for 30 min, diluted with CH_2Cl_2 (200 mL), quenched by the addition of saturated $NaHCO_{3(aq)}$ (50 mL), washed with brine (50 mL), dried (Na_2SO_4), and concentrated in vacuo to provide crude product. The crude product was used directly or purified by crystallization or trituration to yield pure arylsulfonylpiperazines (75% to quantitative).

Preparation of *N*-Aryl-2-((arylsulfonyl)piperazinyl)-acetamides. General Procedure C. Sodium carbonate (0.4 mmol, 2 equiv) or triethylamine (0.4 mmol, 2 equiv) was added to a solution of *N*-aryl-2-bromoacetamide (0.2 mmol, 1 equiv) and arylsulfonylpiperazine (0.2 mmol, 1 equiv) in THF (1 mL, 0.2 M) at 23 °C. The reaction mixture was allowed to stir for 16 h, diluted with CH_2Cl_2 (5 mL), filtered, and concentrated in vacuo to afford crude product. The crude product was purified by flash column chromatography to yield pure *N*-aryl-2-((arylsulfonyl)piperazinyl)-acetamides (48−86%).

2-Bromo-*N*-(2-fluorophenyl)acetamide (2). Following general procedure A, the crude product was precipitated (Et_2O/hexanes) to give pure **2** as a white solid (26%): ^{1}H NMR ($CDCl_3$, 400 MHz) δ = 8.40 (br s, 1H), 8.24 (t, J = 7.8 Hz, 1H), 7.04−7.19 (m, 3H), 4.04 (s, 2H); ^{13}C NMR ($CDCl_3$, 101 MHz) δ = 163.6, 154.1, 151.6, 125.7, 125.6, 125.5, 125.4, 124.7, 121.7, 115.2, 115.0, 29.4; IR (neat) λ_{max} 3313, 1669, 1620, 1330, 1105, 758; HRMS (ESI) m/z calcd for $C_8H_7BrFNNaO$, 253.9587; found, 253.9591.

1-([4-Fluorophenyl]sulfonyl)piperazine (3). Following general procedure B, the crude product was crystallized (EtOAc/hexanes) to give pure **3** as a white solid (93%): ^{1}H NMR ($CDCl_3$, 500 MHz) δ = 7.70−7.79 (m, 2H), 7.16−7.24 (m, 2H), 2.93−3.00 (m, 4H), 2.87−2.93 (m, 4H), 1.52 (s, NH); ^{13}C NMR ($CDCl_3$, 126 MHz) δ = 166.3, 164.3, 131.8, 131.8, 130.5, 130.5, 116.4, 116.2, 46.9, 45.4; IR (neat) λ_{max} 2762, 1592, 1495,1341, 1170, 541, 539. Anal. Calcd for $C_{10}H_{13}FN_2O_2S$: C, 49.17%; H, 5.36%; N, 11.47%. Found: C, 49.04%; H, 5.45%; N, 11.30%. HRMS (ESI) m/z calcd for $C_{10}H_{14}FN_2O_2S$, 245.0755; found, 245.0758.

***N*-(2-Fluorophenyl)-2-(4-((4-fluorophenyl)sulfonyl)-piperazin-1-yl)acetamide (1).** Following general procedure C, the crude product was purified by flash column chromatography (silica, 4:6 EtOAc/hexanes) to provide **1** as a white solid (59%): ^{1}H NMR ($CDCl_3$, 400 MHz) δ = 9.08 (br s, 1H), 8.25 (t, J = 8.0 Hz, 1H), 7.73−7.82 (m, 2H), 7.18−7.28 (m, 2H), 7.04−7.13 (m, 1H), 6.93−7.04 (m, 2H), 3.16 (s, 2H), 3.11 (br s, 4H), 2.69 (t, J = 4.9 Hz, 4H); ^{13}C NMR ($CDCl_3$, 101 MHz) δ = 167.5, 166.7, 164.1, 153.7, 151.2, 131.9, 131.9, 130.5, 130.4, 125.9, 125.8, 124.7, 124.7, 124.6, 124.5, 121.5, 116.6, 116.4, 114.9, 114.7, 61.6, 52.5, 46.1; IR (neat) λ_{max} 3504, 2831, 1699, 1531, 1173, 951, 735, 548. Anal. Calcd for $C_{18}H_{19}F_2N_3O_3S$: C, 54.67%; H, 4.84%; N, 10.63%. Found: C, 54.72%; H, 4.94%; N, 10.44%. HRMS (ESI) m/z calcd for $C_{18}H_{20}F_2N_3O_3S$, 396.1188; found, 396.1173.

2-(4-((4-Fluorophenyl)sulfonyl)piperazin-1-yl)acetic Acid (9). Following general procedure C, using triethylamine, the crude product was purified by crystallization (CH_3OH) to provide **9** as a white crystal (30%): ^{1}H NMR (DMSO-d_6, 500 MHz) δ = 7.80 (dd, J = 8.4, 5.2 Hz, 2H), 7.47 (br t, J = 8.7 Hz, 2H), 3.13 (s, 2H), 2.88 (br s, 4H), 2.58 (br s, 4H); ^{13}C NMR (DMSO-d_6, 126 MHz) δ = 171.2, 165.7, 163.7, 131.2, 131.1, 130.7, 130.6, 116.7, 116.5, 57.8, 50.8, 45.8; IR (neat) λ_{max} 3470, 1634, 1355, 1173, 935, 733, 548; HRMS (ESI) m/z calcd for $C_{12}H_{16}FN_2O_4S$, 303.0809; found, 303.0794.

2-(4-((4-Fluorophenyl)sulfonyl)piperazin-1-yl)-*N*-(1*H*-indazol-5-yl)acetamide (11). EDCI (66.9 mg, 0.349 mmol) was added to a solution of **9** (105.4 mg, 0.349 mmol), 5-aminoindazole (51.1 mg, 0.384 mmol), and HOBt (47.2 mg, 0349 mmol) in DMF (1.7 mL) at 0 °C. The reaction mixture was stirred for 16 h while warming to 23 °C, diluted with CH_2Cl_2 (10 mL), washed with H_2O (3 × 5 mL), brine (5 mL), dried (Na_2SO_4), and concentrated in vacuo to produce a crude brown solid. The crude material was purified by flash column chromatography (silica, 8:2 EtOAc/hexanes) to yield **11** as a white solid (67.7 mg, 46%): ^{1}H NMR (DMSO-d_6, 400 MHz) δ = 12.93 (br s, NH), 9.60 (s, NH), 7.98 (s, 1H), 8.03 (s, 1H), 7.83 (dd, J = 8.7, 5.3 Hz, 2H), 7.50 (t, J = 8.7 Hz, 2H), 7.34−7.46 (m, 2H), 3.14 (s, 2H), 3.00 (br s, 4H), 2.60 (apparent t, J = 4.3 Hz, 4H); ^{13}C NMR (DMSO-d_6, 126 MHz) δ = 167.7, 165.7, 163.7, 137.0, 133.3, 131.5, 131.5, 131.4, 130.7, 130.6, 122.6, 120.9, 116.7, 116.5, 110.5, 109.9, 61.0, 51.6, 45.7; IR (neat) λ_{max} 3628, 1682, 1171, 948, 735, 548. HRMS (ESI) m/z calcd for $C_{19}H_{20}FN_5NaO_3S$, 440.1163; found, 440.1148.

2-(4-((4-Fluorophenyl)sulfonyl)piperazin-1-yl)-*N*-(1H-pyrazol-3-yl)acetamide (12). Following general procedure C, crude product was purified by flash column chromatography (silica, EtOAc) to provide **12** as a white solid (47%): ^{1}H NMR ($CDCl_3$, 500 MHz) δ = 10.50 (br s, NH) 9.15 (s, NH), 7.67−7.82 (m, 2H), 7.40 (d, J = 2.4 Hz, 1H), 7.15−7.30 (m, 2H), 6.64 (d, J = 2.4 Hz, 1H), 3.14 (s, 2H), 3.05 (br s, 4H), 2.65 (br t, J = 4.7 Hz, 4H); ^{13}C NMR ($CDCl_3$, 126 MHz) δ = 167.5, 166.5, 164.4, 146.1, 131.4, 131.4, 130.5, 130.5, 130.1, 116.7, 116.6, 96.7, 61.3, 52.6, 45.9; IR (neat) λ_{max} 3613, 3308, 2938, 2834, 1668, 1592, 1169, 954, 836, 732, 547. Anal. Calcd for $C_{15}H_{18}FN_5O_3S$: C, 49.04%; H, 4.94%. Found: C, 48.07%; H, 5.11%. HRMS (ESI) m/z calcd for $C_{15}H_{19}FN_5O_3S$, 368.1187; found, 368.1170.

2-(4-((4-Fluorophenyl)sulfonyl)piperazin-1-yl)-*N*-(4-methoxyphenyl)acetamide (13). Following general procedure C, crude product was purified by flash column chromatography (silica, 1:1 EtOAc/hexanes) to provide **13** as a white solid (79%): ^{1}H NMR

($CDCl_3$, 400 MHz) δ = 8.53 (s, 1H), 7.73−7.82 (m, 2H), 7.30−7.39 (m, 2H), 7.20−7.28 (m, 2H), 6.77−6.85 (m, 2H), 3.75 (s, 3H), 3.10 (s, 2H), 3.08 (br s, 4H), 2.66 (br t, J = 4.8 Hz, 4H); ^{13}C NMR ($CDCl_3$, 101 MHz) δ = 167.2, 166.6, 164.1, 156.5, 131.8, 131.8, 130.5, 130.4, 130.4, 121.5, 116.7, 116.4, 114.2, 61.6, 55.5, 52.6, 45.9; IR (neat) λ_{max} 2840, 1916, 1683, 1515, 1172, 952, 839, 735, 548. Anal. Calcd for $C_{19}H_{22}FN_3O_4S$: C, 56.01%; H, 5.44%; N, 10.31%. Found: C, 56.29%; H, 5.64%; N, 10.22%. HRMS (ESI) m/z calcd for $C_{19}H_{23}FN_3O_4S$, 408.1388; found, 408.1383.

***N*-(4-Fluorophenyl)-2-(4-((4-fluorophenyl)sulfonyl)-piperazin-1-yl)acetamide (14).** Following general procedure C, crude product was purified by flash column chromatography (silica, 1:1 EtOAc/hexanes) to provide pure **14** as a white solid (86%): ^{1}H NMR ($CDCl_3$, 500 MHz) δ = 8.63 (br s, 1H), 7.69−7.85 (m, 2H), 7.37−7.47 (m, 2H), 7.25 (apparent t, J = 8.5 Hz, 2H), 6.92−7.01 (m, 2H), 3.13 (s, 2H), 3.11 (br s, 4H), 2.69 (t, J = 4.9 Hz, 4H); ^{13}C NMR ($CDCl_3$, 126 MHz) δ = 167.4, 166.5, 164.4, 160.5, 158.5, 133.4, 133.3, 132.0, 132.0, 130.6, 130.5, 121.5, 121.4, 116.7, 116.5, 115.8, 115.7, 61.7, 52.7, 46.0; IR (neat) λ_{max} 2982, 1666, 1523, 1351, 1172, 947, 834, 740, 549. Anal. Calcd for $C_{18}H_{19}F_2N_3O_3S$: C, 54.67%; H, 4.84%; N, 10.63%. Found: C, 55.00%; H, 5.21%; N, 10.47%. HRMS (ESI) m/z calcd for $C_{18}H_{20}F_2N_3O_3S$, 396.1188; found, 396.1177.

2-(4-((4-Fluorophenyl)sulfonyl)piperazin-1-yl)-*N*-phenylacetamide (15). Following general procedure C, crude product was purified by flash column chromatography (silica, 4:6 EtOAc/hexanes) to provide **15** as a white solid (43%): ^{1}H NMR ($CDCl_3$, 500 MHz) δ = 8.65 (br s, 1H), 7.74−7.83 (m, 2H), 7.43−7.50 (m, 2H), 7.19−7.33 (m, 4H), 7.03−7.14 (m, 1H), 3.13 (s, 2H), 3.10 (br s, 4H), 2.68 (t, J = 4.9 Hz, 4H); ^{13}C NMR ($CDCl_3$, 126 MHz) δ = 167.4, 166.4, 164.4, 137.3, 132.0, 131.9, 130.6, 130.5, 129.1, 124.5, 119.7, 116.7, 116.5, 61.8, 52.6, 46.0; IR (neat) λ_{max} 3270, 3059, 2944, 1677, 1524, 1173, 946, 737, 548. Anal. Calcd for $C_{18}H_{20}FN_3O_3S$: C, 57.28%; H, 5.34%; N, 11.13%. Found: C, 57.39%; H, 5.54%; N, 11.00%. HRMS (ESI) m/z calcd for $C_{18}H_{21}FN_3O_3S$, 378.1282; found 378.1270.

***N*-(2-Fluorophenyl)-2-(4-((2-fluorophenyl)sulfonyl)-piperazin-1-yl)acetamide (16).** Following general procedure C, crude product was purified by flash column chromatography (silica, 3:7 EtOAc/hexanes) to provide **16** as a white solid (53%): ^{1}H NMR ($CDCl_3$, 400 MHz) δ = 9.20 (br s, NH), 8.30 (t, J = 8.1 Hz, 1H), 7.80−7.92 (m, 1H), 7.54−7.69 (m, 1H), 7.27−7.35 (m, 1H), 7.23−7.29 (m, 1H), 7.08−7.17 (m, 1H), 6.91−7.08 (m, 2H), 3.26−3.42 (m, 4H), 3.20 (s, 2H), 2.65−2.77 (m, 4H); ^{13}C NMR ($CDCl_3$, 101 MHz) δ = 167.6, 160.3, 157.8, 153.7, 151.3, 135.4, 135.3, 131.3, 125.9, 125.8, 125.4, 125.3, 124.7, 124.7, 124.7, 124.6, 124.6, 124.5, 121.5, 117.6, 117.4, 114.9, 114.7, 61.8, 52.9, 45.8, 45.8; IR (neat) λ_{max} 3308, 2857, 1700, 1185, 766, 736, 586. Anal. Calcd for $C_{18}H_{19}F_2N_3O_3S$: C, 54.67%; H, 4.84%; N, 10.63%. Found: C, 54.82%; H, 4.77%; N, 10.49%. HRMS (ESI) m/z calcd for $C_{18}H_{20}F_2N_3O_3S$, 396.1188; found 396.1168.

***N*-(2-Fluorophenyl)-2-(4-(pyridin-3-ylsulfonyl)piperazin-1-yl)acetamide (17).** Following general procedure C, crude product was purified by flash column chromatography (silica, 8:2 EtOAc/hexanes) to provide **17** as a white solid (66%): ^{1}H NMR ($CDCl_3$, 500 MHz) δ = 9.06 (br s, 1H), 9.00 (dd, J = 2.4, 0.8 Hz, 1H), 8.86 (dd, J = 5.0, 1.6 Hz, 1H), 8.21−8.30 (m, 1H), 8.03−8.10 (m, 1H), 7.52 (ddd, J = 8.0, 4.8, 0.8 Hz, 1H), 7.07−7.12 (m, 1H), 6.96−7.05 (m, 2H), 3.18 (s, 6H), 2.72 (t, J = 4.9 Hz, 4H); ^{13}C NMR ($CDCl_3$, 126 MHz) δ = 167.4, 153.7, 153.4, 151.5, 148.5, 135.4, 132.8, 125.8, 125.7, 124.7, 124.7, 124.6, 124.6, 123.9, 121.5, 114.9, 114.8, 61.7, 52.5, 46.0; IR (neat) λ_{max} 3311, 2830, 1694, 1456, 1176, 953, 756, 583. Anal. Calcd for $C_{17}H_{19}FN_4O_3S$: C, 53.96%; H, 5.06%; N, 14.81%. Found: C, 54.21%; H, 5.22%; N, 14.67%. HRMS (ESI) m/z calcd for $C_{17}H_{20}FN_4O_3S$, 379.1235; found, 379.1236.

***N*-(2-Fluorophenyl)-2-(4-(phenylsulfonyl)piperazin-1-yl)-acetamide (18).** Following general procedure C, crude product was purified by flash column chromatography (silica, 4:6 EtOAc/hexanes) to provide **18** as a white solid (79%): ^{1}H NMR ($CDCl_3$, 500 MHz) δ = 9.09 (br s, NH), 8.26 (t, J = 8.0 Hz, 1H), 7.74−7.80 (m, 2H), 7.60−7.67 (m, 1H), 7.50−7.60 (m, 2H), 7.06−7.15 (m, 1H), 6.91−7.06 (m, 2H), 3.16 (s, 2H), 3.13 (br s, 4H), 2.69 (br t, J = 4.9 Hz, 4H); ^{13}C NMR ($CDCl_3$, 126 MHz) δ = 167.6, 153.4, 151.5, 135.9, 133.1, 129.2, 127.7, 125.9, 125.8, 124.7, 124.7, 124.6, 124.5, 121.5, 114.9, 114.7, 61.7, 52.6, 46.1; IR (neat) λ_{max} 3302, 2829, 1918, 1693, 1172, 952, 743, 568. Anal. Calcd for $C_{18}H_{20}FN_3O_3S$: C, 57.28%; H, 5.34%; N, 11.13%. Found: C, 57.61%; H, 5.51%; N, 11.16%. HRMS (ESI) m/z calcd for $C_{18}H_{21}FN_3O_3S$, 378.1282; found, 378.1272.

***N*-(2-Fluorophenyl)-2-(4-((4-methoxyphenyl)sulfonyl)-piperazin-1-yl)acetamide (19).** Following general procedure C, crude product was purified by flash column chromatography (silica, 1:1 EtOAc/hexanes) to provide **19** as a white solid (77%): ^{1}H NMR ($CDCl_3$, 500 MHz) δ = 9.07 (br s, 1H), 8.23 (t, J = 7.9 Hz, 1H), 7.61−7.70 (m, 2H), 7.01−7.09 (m, 1H), 6.95−7.01 (m, 4H), 3.85 (s, 4H), 3.13 (s, 2H), 3.06 (br s, 4H), 2.65 (br t, J = 4.9 Hz, 4H); ^{13}C NMR ($CDCl_3$, 126 MHz) δ = 167.6, 163.2, 153.4, 151.4, 129.8, 127.2, 125.8, 125.7, 124.5, 124.5, 124.4, 124.4, 121.5, 114.8, 114.6, 114.3, 61.5, 55.6, 52.4, 46.0; IR (neat) λ_{max} 2843, 1953, 1699, 1164, 949, 735, 559. Anal. Calcd for $C_{19}H_{22}FN_3O_4S$: C, 56.01%; H, 5.44%; N, 10.31%. Found: C, 56.20%; H, 5.64%; N, 10.17%. HRMS (ESI) m/z calcd for $C_{19}H_{23}FN_3O_4S$, 408.1388; found, 408.1390.

***N*-(4-Fluorophenyl)-2-(4-((2-fluorophenyl)sulfonyl)-piperazin-1-yl)acetamide (20).** Following general procedure C, crude product was purified by flash column chromatography (silica, 4:6 EtOAc/hexanes) to provide **20** as a white solid (86%): ^{1}H NMR ($CDCl_3$, 500 MHz) δ = 8.73 (br s, 1H), 7.75−7.87 (m, 1H), 7.54−7.64 (m, 1H), 7.39−7.47 (m, 2H), 7.26−7.31 (m, 1H), 7.17−7.25 (m, 1H), 6.90−7.00 (m, 2H), 3.28 (br s, 4H), 3.12 (s, 2H), 2.48−2.70 (br t, 4H); ^{13}C NMR ($CDCl_3$, 126 MHz) δ = 167.4, 160.3, 160.0, 158.4, 157.9, 135.4, 135.3, 133.4, 131.2, 125.3, 125.1, 124.7, 124.6, 121.4, 121.4, 117.5, 117.3, 115.7, 115.5, 61.6, 52.8, 45.6, 45.6; IR (neat) λ_{max} 3403, 2839, 1690, 1177, 950, 836, 739, 584. Anal. Calcd for $C_{18}H_{19}F_2N_3O_3S$: C, 54.67%; H, 4.84%; N, 10.63%. Found: C, 54.79%; H, 5.17%; N, 10.64%. HRMS (ESI) m/z calcd for $C_{18}H_{20}F_2N_3O_3S$, 396.1188; found, 396.1183.

2-(4-((2-Fluorophenyl)sulfonyl)piperazin-1-yl)-*N*-(4-methoxyphenyl)acetamide (21). Following general procedure C, crude product was purified by flash column chromatography (silica, 4:6 EtOAc/hexanes) to provide **21** as a white solid (89%): ^{1}H NMR ($CDCl_3$, 500 MHz) δ = 8.61 (br s, NH), 7.74−7.82 (m, 1H), 7.49−7.59 (m, 1H), 7.31−7.38 (m, 2H), 7.22−7.28 (m, 1H), 7.19 (t, J = 9.3 Hz, 1H), 6.69−6.82 (m, 2H), 3.70 (s, 3H), 3.23 (br s, 4H), 3.07 (s, 2H), 2.48−2.65 (br t, 4H); ^{13}C NMR ($CDCl_3$, 126 MHz) δ = 167.2, 159.9, 157.8, 156.4, 135.3, 135.2, 131.1, 130.4, 125.1, 125.0, 124.6, 124.5, 121.4, 117.4, 117.2, 114.0, 61.5, 55.4, 52.7, 45.6; IR (neat) λ_{max} 3313, 2939, 1686, 1598, 1514, 1174, 955, 828, 734. Anal. Calcd for $C_{19}H_{22}FN_3O_4S$: C, 56.01%; H, 5.44%; N, 10.31%. Found: C, 55.53%; H, 5.70%; N, 10.07%. HRMS (ESI) m/z calcd for $C_{19}H_{23}FN_3O_4S$, 408.1388; found, 408.1390.

Methyl 4-(2-(4-((2-Fluorophenyl)sulfonyl)piperazin-1-yl)-acetamido)benzoate (22). Following general procedure C, crude product was purified by flash column chromatography (silica, 1:1 EtOAc/hexanes) to provide **22** as a white solid (80%): ^{1}H NMR ($CDCl_3$, 500 MHz) δ = 8.95 (br s, NH), 7.97 (d, J = 8.5 Hz, 2H), 7.85 (t, J = 6.8 Hz, 1H), 7.59−7.69 (m, 1H), 7.57 (d, J = 8.5 Hz, 2H), 7.31 (t, J = 7.6 Hz, 1H), 7.15−7.28 (m, 1H), 3.88 (s, 3H), 3.32 (br s, 4H), 3.17 (s, 2H), 2.57−2.76 (m, 4H); ^{13}C NMR ($CDCl_3$, 126 MHz) δ = 167.9, 166.5, 160.1, 158.0, 141.4, 135.4, 135.4, 131.3, 130.9, 125.9, 125.5, 125.4, 124.7, 124.7, 118.8, 117.6, 117.4, 61.9, 53.0, 52.1, 45.7; IR (neat) λ_{max} 3282, 1702, 1598, 1281, 1175, 954, 733, 584. Anal. Calcd for $C_{20}H_{22}FN_3O_5S$: C, 55.16%; H, 5.09%; N, 9.65%. Found: C, 55.15%; H, 5.31%; N, 9.43%. HRMS (ESI) m/z calcd for $C_{20}H_{23}FN_3O_5S$, 436.1337; found, 436.1350.

4-(2-(4-((2-Fluorophenyl)sulfonyl)piperazin-1-yl)acetamido)-benzoic Acid (23). Following general procedure C, crude product was purified by flash column chromatography (silica, 3% MeOH/EtOAc) to provide **23** a white solid (44%): ^{1}H NMR (DMSO-d_6, 500 MHz) δ = 12.66 (br s, NH), 9.91 (s, NH), 7.87 (d, J = 8.7 Hz, 2H), 7.74−7.83 (m, 2H), 7.71 (d, J = 8.7 Hz, 2H), 7.46−7.53 (m, 1H), 7.44 (t, J = 7.6 Hz, 1H), 3.19 (s, 2H), 3.14 (br s, 4H), 2.60 (br s, 4H); ^{13}C NMR (DMSO-d_6, 126 MHz) δ = 168.5, 166.9, 159.3, 157.3, 142.5, 136.1, 136.0, 130.9, 130.2, 125.5, 125.2, 125.2, 124.0, 123.9, 118.9,

117.7, 117.5, 61.0, 51.8, 45.4; IR (neat) λ_{max} 2924, 2854, 1707, 1600, 1174, 952, 733, 584. Anal. Calcd for $C_{19}H_{20}FN_3O_5S$: C, 54.15%; H, 4.78%; N, 9.97%. Found: C, 54.52%; H, 5.20%; N, 9.40%. HRMS (ESI) m/z calcd for $C_{19}H_{21}FN_3O_5S$, 422.1180; found, 422.1162.

2-(4-((2-Fluorophenyl)sulfonyl)piperazin-1-yl)-*N*-(1H-pyrazol-3-yl)acetamide (24). Following general procedure C, crude product was purified by flash column chromatography (silica, EtOAc) to provide **24** as a white solid (48%): ^{1}H NMR ($CDCl_3$, 400 MHz) δ = 10.57 (br s, NH), 9.23 (s, NH), 7.75−7.86 (m, 1H), 7.54−7.66 (m, 1H), 7.41 (d, J = 2.3 Hz, 1H), 7.26−7.33 (m, 1H), 7.18−7.25 (m, 1H), 6.63 (d, J = 2.3 Hz, 1H), 3.23 (br s, 4H), 3.14 (s, 2H), 2.64 (br t, J = 4.9 Hz, 4H); ^{13}C NMR ($CDCl_3$, 101 MHz) δ = 167.5, 160.3, 157.7, 146.1, 135.5, 135.4, 131.3, 130.2, 124.8, 124.7, 124.7, 117.7, 117.5, 96.6, 61.4, 52.8, 45.7; IR (neat) λ_{max} 3212, 1668, 1567, 1176, 735, 583. HRMS (ESI) m/z calcd for $C_{15}H_{19}FN_5O_3S$: 368.1187; found, 368.1173.

***N*-(1*H*-Pyrazol-3-yl)-2-(4-(pyridin-3-ylsulfonyl)piperazin-1-yl)acetamide (25).** Following general procedure C, crude product was purified by flash column chromatography (silica, 4% MeOH/EtOAc) to provide **25** as a white solid (34%): ^{1}H NMR ($CDCl_3$, 500 MHz) δ = 9.12 (s, NH), 8.99 (d, J = 1.9 Hz, 1H), 8.87 (dd, J = 4.7, 1.6 Hz, 1H), 8.05 (dt, J = 8.1, 1.9 Hz, 1H), 7.49−7.59 (m, 1H), 7.44 (d, J = 2.5 Hz, 1H), 6.67 (d, J = 2.5 Hz, 1H), 3.16 (s, 2H), 3.14 (br s, 4H), 2.69 (br t, J = 4.7 Hz, 4H); ^{13}C NMR ($CDCl_3$, 126 MHz) δ = 167.3, 153.7, 148.5, 146.2, 135.5, 132.6, 130.2, 124.0, 96.8, 61.4, 52.6, 45.9; IR (neat) λ_{max} 3608, 3240, 2947, 2829, 1683, 1176, 951, 757, 583. Anal. Calcd for $C_{14}H_{18}N_6O_3S$: C, 47.99%; H, 5.18%; N, 23.98%. Found: C, 47.61%; H, 5.54%; N, 22.48%. HRMS (ESI) m/z calcd for $C_{14}H_{19}N_6O_3S$, 351.1234; found, 351.1216.

***N*-(4-Methoxyphenyl)-2-(4-(pyridin-3-ylsulfonyl)piperazin-1-yl)acetamide (26).** Following general procedure C, crude product was purified by flash column chromatography (silica, 9:1 EtOAc/hexanes) to provide **26** as a white solid (59%): ^{1}H NMR ($CDCl_3$, 500 MHz) δ = 8.98 (d, J = 2.2 Hz, 1H), 8.84 (dd, J = 4.8, 1.1 Hz, 1H), 8.50 (s, NH), 8.04 (dd, J = 8.2, 1.6 Hz, 1H), 7.50 (dd, J = 7.9, 4.8 Hz, 1H), 7.34 (d, J = 9.0 Hz, 2H), 6.80 (d, J = 9.0 Hz, 2H), 3.74 (s, 3H), 3.14 (br s, 4H), 3.11 (s, 2H), 2.68 (br t, J = 4.9 Hz, 4H); ^{13}C NMR ($CDCl_3$, 126 MHz) δ = 167.0, 156.6, 153.7, 148.5, 135.4, 132.8, 130.4, 123.9, 121.5, 114.2, 61.6, 55.5, 52.5, 45.9; IR (neat) λ_{max} 3320, 2834, 1679, 1514, 1175, 951, 756, 583. Anal. Calcd for $C_{18}H_{22}N_4O_4S$: C, 55.37%; H, 5.68%; N, 14.35%. Found: C, 55.50%; H, 5.95%; N, 13.85%. HRMS (ESI) m/z calcd for $C_{18}H_{23}N_4O_4S$, 391.1435; found, 391.1439.

***N*-Phenyl-2-(4-(phenylsulfonyl)piperazin-1-yl)acetamide (27).** Following general procedure C, crude product was purified by flash column chromatography (silica, 4:6 EtOAc/hexanes) to provide **27** as a white solid (70%): ^{1}H NMR ($CDCl_3$, 500 MHz) δ = 8.66 (br s, NH), 7.77 (d, J = 7.6 Hz, 2H), 7.64 (t, J = 7.6 Hz, 1H), 7.57 (t, J = 7.6 Hz, 2H), 7.45 (d, J = 7.6 Hz, 2H), 7.28 (t, J = 7.6 Hz, 2H), 7.08 (t, J = 7.6 Hz, 1H), 3.11 (s, 6H), 2.67 (br t, J = 4.7 Hz, 4H); ^{13}C NMR ($CDCl_3$, 126 MHz) δ = 167.4, 137.3, 135.8, 133.1, 129.3, 129.0, 127.8, 124.5, 119.6, 61.7, 52.6, 45.9; IR (neat) λ_{max} 3283, 2848, 1674, 1523, 1176, 945, 745, 694, 580. Anal. Calcd for $C_{18}H_{21}N_3O_3S$: C, 60.15%; H, 5.89%; N, 11.69%. Found: C, 60.23%; H, 6.08%; N, 11.80%. HRMS (ESI) m/z calcd for $C_{18}H_{22}N_3O_3S$, 360.1376; found, 360.1361.

***N*-(4-Fluorophenyl)-2-(4-((4-methoxyphenyl)sulfonyl)-piperazin-1-yl)acetamide (28).** Following general procedure C, crude product was purified by flash column chromatography (silica, 1:1 EtOAc/hexanes) to provide **28** as a white solid (77%): ^{1}H NMR ($CDCl_3$, 500 MHz) δ = 8.76 (br s, 1H), 7.61−7.72 (m, J = 8.8 Hz, 2H), 7.41 (dd, J = 8.7, 4.6 Hz, 2H), 6.97−7.03 (m, J = 8.8 Hz, 2H), 6.94 (t, J = 8.7 Hz, 2H), 3.85 (s, 3H), 3.14 (br s, 2H), 3.07 (br s, 4H), 2.69 (br s, 4H); ^{13}C NMR ($CDCl_3$, 101 MHz) δ = 167.4, 163.3, 160.6, 158.2, 133.4, 133.4, 129.9, 127.2, 121.5, 121.4, 115.8, 115.5, 114.4, 77.3, 61.5, 55.7, 52.6, 45.9; IR (neat) λ_{max} 3312, 2842, 1686, 1510, 1163, 949, 835, 735. Anal. Calcd for $C_{19}H_{22}FN_3O_4S$: C, 56.01%; H, 5.44%; N, 10.31%. Found: C, 57.30%; H, 5.73%; N, 10.32%. HRMS (ESI) m/z calcd for $C_{19}H_{23}FN_3O_4S$, 408.1388; found, 408.1394.

***N*-([1,1′-Biphenyl]-2-yl)-2-(4-((4-fluorophenyl)sulfonyl)-piperazin-1-yl)acetamide (29).** Following general procedure C, crude product was purified by flash column chromatography (silica, 4:6 EtOAc/hexanes) to provide **29** as a white solid (83%): ^{1}H NMR ($CDCl_3$, 500 MHz) δ = 7.68−7.80 (m, 2H), 7.28−7.41 (m, 8H), 7.15−7.23 (m, 2H), 7.09 (dd, J = 7.7, 1.1 Hz, 1H), 3.22 (s, 2H), 2.97 (br s, 4H), 2.44 (br t, J = 4.9 Hz, 4H); ^{13}C NMR ($CDCl_3$, 126 MHz) δ = 168.3, 166.3, 164.3, 147.5, 137.6, 135.1, 131.5, 131.5, 130.9, 130.6, 130.5, 129.0, 128.7, 128.4, 127.6, 126.6, 122.5, 116.4, 116.3, 58.6, 51.5, 45.8; IR (neat) λ_{max} 3448, 1771, 1592, 1155, 1139, 737, 548. Anal. Calcd for $C_{24}H_{23}FN_2O_4S$: C, 63.42%; H, 5.10%; N, 6.16%. Found: C, 60.69%; H, 5.16%; N, 5.97%. HRMS (ESI) m/z calcd for $C_{24}H_{24}FN_2O_4S$, 455.1435; found, 455.1444.

***N*-([1,1′-Biphenyl]-2-yl)-2-(4-((2-fluorophenyl)sulfonyl)-piperazin-1-yl)acetamide (30).** Following general procedure C, crude product was purified by flash column chromatography (silica, 4:6 EtOAc/hexanes) to provide **30** as a white solid (84%): ^{1}H NMR ($CDCl_3$, 500 MHz) δ = 7.77−7.83 (m, 1H), 7.51−7.60 (m, 1H), 7.28−7.41 (m, 8H), 7.23−7.28 (m, 1H), 7.19 (td, J = 9.2, 0.8 Hz, 1H), 7.06−7.12 (m, 1H), 3.24 (s, 2H), 3.14 (br t, 4H), 2.43 (br t, 4H); ^{13}C NMR ($CDCl_3$, 126 MHz) δ = 168.3, 160.1, 158.1, 147.5, 137.6, 135.2, 135.2, 135.1, 131.4, 130.9, 129.0, 128.7, 128.3, 127.6, 126.6, 124.7, 124.6, 124.5, 124.5, 122.5, 117.5, 117.3, 58.7, 51.8, 45.6; IR (neat) λ_{max} 3370, 2860, 1770, 1599, 1130, 739, 584. Anal. Calcd for $C_{24}H_{23}FN_2O_4S$: C, 63.42%; H, 5.10%; N, 6.16%. Found: C, 61.95%; H, 5.20%; N, 5.98%. HRMS (ESI) m/z calcd for $C_{24}H_{24}FN_2O_4S$, 455.1435; found, 455.1433.

■ ASSOCIATED CONTENT

Ⓢ Supporting Information

Experimental procedures and characterization data of precursors of compounds **12**−**30**; NMR spectra. This material is available free of charge via the Internet at http://pubs.acs.org.

■ AUTHOR INFORMATION

Corresponding Author

*Telephone: (614) 292-3771. Telefax: (614) 292-9083. E-mail: Mckay.2@osu.edu.

■ ACKNOWLEDGMENTS

All stably transfected human cell lines were kindly provided by Dr. Jon M. Lindstrom, Department of Neuroscience School of Medicine, University of Pennsylvania, Philadelphia, PA. This work was supported by the National Institutes of Health National Institute on Drug Abuse (Grant DA029433). Financial support for B.J.H. is from the National Institutes of Health National Institute on Drug Abuse Diversity Supplement. Financial support for R.E.P. is from an American Chemical Society Predoctoral Fellowship in Medicinal Chemistry. We thank OBIC for funding for a Bruker MicrOTOF mass spectrometer. We thank Karl Werbovetz, Ph.D., and Rostislav Likhotvorik for their help preparing this manuscript.

■ ABBREVIATIONS USED

NAM, negative allosteric modulator; nAChR, neuronal nicotinic acetylcholine receptor; HBK, HEPES-buffered Krebs; SAR, structure−activity relationship; n_h, Hill coefficient; SBVS, structure-based virtual screening

■ REFERENCES

(1) Lloyd, G. K.; Williams, M. Neuronal nicotinic acetylcholine receptors as novel drug targets. *J. Pharmacol. Exp. Ther.* **2000**, *292*, 461−467.

(2) Schuller, H. M. Is cancer triggered by altered signalling of nicotinic acetylcholine receptors? *Nat. Rev. Cancer* **2009**, *9*, 195−205.

(3) Improgo, M. R. D.; Scofield, M. D.; Tapper, A. R.; Gardner, P. D. The nicotinic acetylcholine receptor CHRNA5/A3/B4 gene cluster:

dual role in nicotine addiction and lung cancer. *Prog. Neurobiol.* **2010**, *92*, 212−226.
(4) Gotti, C.; Riganti, L.; Vailati, S.; Clementi, F. Brain neuronal nicotinic receptors as new targets for drug discovery. *Curr. Pharm. Des.* **2006**, *12*, 407−428.
(5) Rice, M. E.; Cragg, S. J. Nicotine amplifies reward-related dopamine signals in striatum. *Nat. Neurosci.* **2004**, *7*, 583−584.
(6) Cooper, E.; Couturier, S.; Ballivet, M. Pentameric structure and subunit stoichiometry of a neuronal nicotinic acetylcholine receptor. *Nature* **1991**, *350*, 235−238.
(7) Anand, R.; Conroy, W. G.; Schoepfer, R.; Whiting, P.; Lindstrom, J. Neuronal nicotinic acetylcholine receptors expressed in *Xenopus* oocytes have a pentameric quaternary structure. *J. Biol. Chem.* **1991**, *266*, 11192−11198.
(8) Lukas, R. J.; Changeux, J.-P.; le Novère, N.; Albuquerque, E. X.; Balfour, D. J. K.; Berg, D. K.; Bertrand, D.; Chiappinelli, V. A.; Clarke, P. B. S.; Collins, A. C.; Dani, J. A.; Grady, S. R.; Kellar, K. J.; Lindstrom, J. M.; Marks, M. J.; Quik, M.; Taylor, P. W.; Wonnacott, S. International Union of Pharmacology. XX. Current status of the nomenclature for nicotinic acetylcholine receptors and their subunits. *Pharmacol. Rev.* **1999**, *51*, 397−401.
(9) Jensen, A. A.; Frolund, B.; Liljefors, T.; Krogsgaard-Larsen, P. Neuronal nicotinic acetylcholine receptors: structural revelations, target identifications, and therapeutic inspirations. *J. Med. Chem.* **2005**, *48*, 4705−4745.
(10) Albuquerque, E. X.; Pereira, E. F. R.; Alkondon, M.; Rogers, S. W. Mammalian nicotinic acetylcholine receptors: from structure to function. *Physiol. Rev.* **2009**, *89*, 73−120.
(11) Tapper, A. R.; McKinney, S. L.; Nashmi, R.; Schwarz, J.; Deshpande, P.; Labarca, C.; Whiteaker, P.; Marks, M. J.; Collins, A. C.; Lester, H. A. Nicotine activation of α4* receptors: sufficient for reward, tolerance, and sensitization. *Science* **2004**, *306*, 1029−1032.
(12) Picciotto, M. R.; Zoli, M.; Rimondini, R.; Léna, C.; Marubio, L. M.; Pich, E. M.; Fuxe, K.; Changeux, J.-P. Acetylcholine receptors containing the β2 subunit are involved in the reinforcing properties of nicotine. *Nature* **1998**, *391*, 173−177.
(13) Knight, C.; Howard, P.; Baker, C. L.; Marton, J. P. The cost-effectiveness of an extended course (12 + 12 weeks) of varenicline compared with other available smoking cessation strategies in the United States: an extension and update to the BENESCO Model. *Value Health* **2009**, *13*, 209−214.
(14) Mihalak, K. B.; Carroll, F. I.; Luetje, C. W. Varenicline is a partial agonist at $\alpha4\beta2$ and a full agonist at $\alpha7$ neuronal nicotinic receptors. *Mol. Pharmacol.* **2006**, *70*, 801−805.
(15) Rollema, H.; Chambers, L. K.; Coe, J. W.; Glowa, J.; Hurst, R. S.; Lebel, L. A.; Lu, Y.; Mansbach, R. S.; Mather, R. J.; Rovetti, C. C.; Sands, S. B.; Schaeffer, E.; Schulz, D. W.; Tingley, F. D.; Williams, K. E. Pharmacological profile of the $\alpha4\beta2$ nicotinic acetylcholine receptor partial agonist varenicline, an effective smoking cessation aid. *Neuropharmacology* **2007**, *52*, 985−994.
(16) Fiore, M. C.; McCarthy, D. E.; Jackson, T. C.; Zehner, M. E.; Jorenby, D. E.; Mielke, M.; Smith, S. S.; Guiliani, T. A.; Baker, T. B. Integrating smoking cessation treatment into primary care: an effectiveness study. *Prev. Med.* **2004**, *38*, 412−420.
(17) Taly, A.; Corringer, P.-J.; Guedin, D.; Lestage, P.; Changeux, J.-P. Nicotinic receptors: allosteric transitions and therapeutic targets in the nervous system. *Nat. Rev. Drug Discovery* **2009**, *8*, 733−750.
(18) Grady, S. R.; Drenan, R. M.; Breining, S. R.; Yohannes, D.; Wageman, C. R.; Fedorov, N. B.; McKinney, S.; Whiteaker, P.; Bencherif, M.; Lester, H. A.; Marks, M. J. Structural differences determine the relative selectivity of nicotinic compounds for native $\alpha4\beta2$*-, $\alpha6\beta2$*-, $\alpha3\beta4$*-, and $\alpha7$-nicoine acetylcholine receptors. *Neuropharmacology* **2010**, *58*, 1054−1066.
(19) López-Hernández, G. Y.; Thinschmidt, J. S.; Zheng, G.; Zhang, Z.; Crooks, P. A.; Dwoskin, L. P.; Papke, R. L. Selective inhibition of acetylcholine-evoked responses of $\alpha7$ neuronal nicotinic acetylcholine receptors by novel tris- and tetrakis-azaaromatic quaternary ammonium antagonists. *Mol. Pharmacol.* **2009**, *76*, 652−666.
(20) Yoshimura, R. F.; Hogenkamp, D. J.; Li, W. Y.; Tran, M. B.; Belluzzi, J. D.; Whittemore, E. R.; Leslie, F. M.; Gee, K. W. Negative allosteric modulation of nicotinic acetylcholine receptors blocks nicotine self-administration in rats. *J. Pharmacol. Exp. Ther.* **2007**, *323*, 907−915.
(21) Weltzin, M. M.; Schulte, M. K. Pharmacological characterization of the allosteric modulator desformylflustrabromine and its interaction with $\alpha4\beta2$ neuronal nicotinic acetylcholine receptor orthosteric ligands. *J. Pharmacol. Exp. Ther.* **2010**, *334*, 917−926.
(22) Hansen, S. B.; Taylor, P. Galanthamine and non-competitive inhibitor binding to ACh-binding protein: evidence for a binding site on non-α-subunit interfaces of heteromeric neuronal nicotinic receptors. *J. Mol. Biol.* **2007**, *369*, 895−901.
(23) Rose, J. E.; Behm, F. M.; Westman, E. C.; Levin, E. D.; Stein, R. M.; Ripka, G. V. Mecamylamine combined with nicotine skin patch facilitates smoking cessation beyond nicotine patch treatment alone. *Clin. Pharmacol. Ther.* **1994**, *56*, 86−99.
(24) Watkins, S. S.; Epping-Jordan, M. P.; Koob, G. F.; Markou, A. Blockade of nicotine self-administration with nicotinic antagonists in rats. *Pharmacol., Biochem. Behav.* **1999**, *62*, 743−751.
(25) Henderson, B. J.; Pavlovicz, R. E.; Allen, J. D.; Gonzalez-Cestari, T. F.; Orac, C. M.; Bonnell, A. B.; Zhu, M. X.; Boyd, R. T.; Li, C.; Bergmeier, S. C.; McKay, D. B. Negative allosteric modulators that target human $\alpha4\beta2$ neuronal nicotinic receptors. *J. Pharmacol. Exp. Ther.* **2010**, *334*, 761−774.
(26) Pavlovicz, R. E.; Henderson, B. J.; Bonnell, A. B.; Boyd, R. T.; McKay, D. B.; Li, C. Identification of a novel negative allosteric site on human $\alpha4\beta2$ and $\alpha3\beta4$ neuronal nicotinic acetylcholine receptors. *PLoS One* **2011**, *6* (9), e24949.
(27) Mahasenan, K. V.; Pavlovicz, R. E.; Henderson, B. J.; González-Cestari, T. F.; Yi, B.; McKay, D. B.; Li, C. Discovery of novel $\alpha4\beta2$ neuronal nicotinic receptor modulators through structure-based virtual screening. *ACS Med. Chem. Lett.* **2011**, *2*, 855−860.
(28) Wang, Z.; Wu, B.; Kuhen, K. L.; Bursulaya, B.; Nguyen, T. N.; Nguyen, D. G.; He, Y. Synthesis and biological evaluations of sulfanyltriazoles as novel HIV-1 non-nuleoside reverse transcriptase inhibitors. *Bioorg. Med. Chem. Lett.* **2006**, *16*, 4174−4177.
(29) Xie, H.; Ng, D.; Savinov, S. N.; Dey, B.; Kwong, P. D.; Wyatt, R.; Smith, A. B.; Hendrickson, W. A. Structure−activity relationships in the binding of chemically derivatized CD4 to gp120 from human immunodeficiency virus. *J. Med. Chem.* **2007**, *50*, 4898−4908.
(30) de Castro Barbosa, M. L.; de Albequerque Melo, G. M.; da Silva, Y. K. C.; de Oliveira Lopes, R.; de Souza, E. T.; de Queiroz, A. C.; Smaniotto, S.; Alexandre-Moreira, M. S.; Barreiro, E. J.; Lima, L. M. Synthesis and pharmacological evaluation of *N*-phenyl-acetamide sulfonamides designed as novel non-hepatotoxic analgesic candidates. *Eur. J. Med. Chem.* **2009**, *44*, 3612−3620.
(31) Carpino, L. A.; El-Fahm, A. The diisopropylcarbodiimide/1-hydroxy-7-azabenzotriazole system: segment coupling and stepwise peptide assembly. *Tetrahedron* **1999**, *55*, 6813−6830.
(32) McKay, D. B.; Chang, C.; González-Cestari, T. F.; McKay, S. B.; El-Hajj, R. A.; Bryant, D. L.; Zhu, D. L.; Swaan, P. W.; Arason, K. M.; Pulipaka, A. B.; Orac, C. M.; Bergmeier, S. C. Analogs of methyllycaconitine as novel noncompetitive inhibitors of nicotinic receptors: pharmacological characterization, computational modeling, and pharmacophore development. *Mol. Pharmacol.* **2007**, *71*, 1288−1297.
(33) González-Cestari, T. F.; Henderson, B. J.; Pavlovicz, R. E.; McKay, S. B.; El-Hajj, R. A.; Pulipaka, A. B.; Orac, C. M.; Reed, D. D.; Boyd, R. T.; Zhu, M. X.; Li, C.; Bergmeier, S. C.; McKay, D. B. Effect of novel negative allosteric modulators of neuronal nicotinic receptors on cells expressing native and recombinant nicotinic receptors: implications for drug discovery. *J. Pharmacol. Exp. Ther.* **2009**, *328*, 504−515.